

This is the accepted manuscript made available via CHORUS. The article has been published as:

## Bounds on Invisible Higgs Boson Decays Extracted from LHC $t\bar{t}H$ Production Data

Ning Zhou, Zepoor Khechadorian, Daniel Whiteson, and Tim M. P. Tait

Phys. Rev. Lett. **113**, 151801 — Published 10 October 2014

DOI: [10.1103/PhysRevLett.113.151801](https://doi.org/10.1103/PhysRevLett.113.151801)

# Bounds on Invisible Higgs boson Decays from $t\bar{t}H$ Production

Ning Zhou,<sup>1</sup> Zepoor Khechadorian,<sup>1</sup> Daniel Whiteson,<sup>1</sup> and Tim M.P. Tait<sup>1</sup>

<sup>1</sup>*Department of Physics and Astronomy, University of California, Irvine, CA 92697*

We present an upper bound on the branching fraction of the Higgs boson to invisible particles, by recasting a CMS search for stop quarks decaying to  $t\bar{t} + E_T^{\text{miss}}$ . The observed (expected) bound,  $\text{BF}(H \rightarrow \text{inv.}) < 0.40(0.65)$  at 95% CL, is the strongest direct limit to date, benefiting from a downward fluctuation in the CMS data in that channel. In addition, we combine this new constraint with existing published constraints to give an observed (expected) bound of  $\text{BF}(H \rightarrow \text{inv.}) < 0.40(0.40)$  at 95% CL, and show some of the implications for theories of dark matter which communicate through the Higgs portal.

PACS numbers:

The particle nature of dark matter stands as one of the most pressing open questions in modern physics. The discovery of the Higgs boson [1, 2] creates a new opportunity to probe this question. Despite the accumulation of evidence which suggests the Higgs boson has Standard Model (SM) properties, decays of the Higgs directly into dark matter particles with order one probabilities remain consistent with experimental measurements.

Interactions between the Higgs boson and dark matter particles exist in a broad set of theories of physics beyond the standard model, including supersymmetric extensions in which Higgs bosons decay to neutralinos [3], models in which the Higgs boson mediates an interaction between dark matter particles and SM particles [4–7], models of graviscalars [8] and models where the Higgs boson plays an important role in the early Universe [9].

Direct experimental searches for invisible decays constrain the invisible branching fraction. The ATLAS experiment searched for  $Vh \rightarrow jj + E_T^{\text{miss}}$ ,  $V = W, Z$  [10]; see Fig 1a. Stronger limits come from the ATLAS  $Zh \rightarrow \ell\ell + E_T^{\text{miss}}$  mode, giving  $\text{BF}(H \rightarrow \text{inv.}) < 0.75$  at 95% CL [11]. The strongest limits currently come from CMS, which uses the  $Zh \rightarrow \ell\ell + E_T^{\text{miss}}$ ,  $Zh \rightarrow b\bar{b} + E_T^{\text{miss}}$  and vector-boson-fusion mode  $qqH \rightarrow jj + E_T^{\text{miss}}$  (Fig 1b) to achieve a constraint of  $\text{BF}(H \rightarrow \text{inv.}) < 0.58$  at 95% CL [12].

The LEP experiments placed constraints for Higgs bosons below  $m_H = 118$  GeV [13], and indirect constraints at the level of  $\text{BF}(H \rightarrow \text{inv.}) < 0.13\text{--}0.19$  [14–16] are available from studies of the visible decay modes [17]. These are typically stronger than direct constraints, but rely on imposing specific assumptions about the coupling to various visible particles which are not currently required by data (otherwise no useful bound on  $\text{BF}(H \rightarrow \text{inv.})$  is obtained [14]). Clearly, direct limits on the branching ratio to invisible modes offer important information that circumvents such theoretical bias.

In this Letter, we report the first direct phenomenological limits using the  $t\bar{t}H$  production mode. The final state of  $t\bar{t} + E_T^{\text{miss}}$  has been studied by CMS in

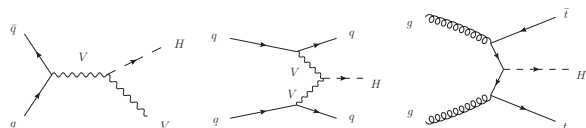


FIG. 1: Diagrams for the production modes used in searches for invisible decay of the Higgs boson. Left, the  $VH$  mode; center, the vector-boson-fusion mode; and right, the  $t\bar{t}H$  mode considered here.

the context of a search for supersymmetric top quarks ( $\tilde{t} \rightarrow bW + E_T^{\text{miss}}$ ) [18]; we demonstrate that these data provide powerful bounds on the invisible Higgs boson branching fraction. In addition, we combine all available direct experimental results into a global LHC result.

The CMS analysis searches for both  $\tilde{t} \rightarrow t\tilde{\chi}_1^0 \rightarrow bW\tilde{\chi}_1^0$  and  $\tilde{t} \rightarrow b\tilde{\chi}^+ \rightarrow bW\tilde{\chi}_1^0$ , both of which give a final state of  $bWbW + E_T^{\text{miss}}$ . The search uses the single-lepton mode, requiring that events have exactly one electron or muon, at least three jets (at least one of which is  $b$ -tagged), and the transverse mass of lepton and  $E_T^{\text{miss}}$  system  $M_T > 120$  GeV. Each of the two searches is divided into low- $\Delta M$  ( $\equiv m_{\tilde{t}} - m_{\tilde{\chi}_1^0}$ ) and high- $\Delta M$  categories, which are further subdivided into four  $E_T^{\text{miss}}$  thresholds optimized to target various mass regions. In all, there are sixteen signal regions. Some include requirements on  $\min(\Delta\phi[E_T^{\text{miss}}, j])$ , the minimum angle between the  $E_T^{\text{miss}}$  and any jet;  $M_{T2}^W$ , the minimal particle mass compatible with all the transverse momentum and mass-shell constraints of  $t\bar{t}$  topology as defined in Ref. [19]; or  $\chi_{\text{had}}^2$ , the compatibility of a triplet of jets with the  $t \rightarrow Wb \rightarrow qq\bar{b}$  decay hypothesis.

We apply the results of the CMS  $\tilde{t}$  search to invisible Higgs boson decays by calculating the expected yield of  $t\bar{t}H$  in each of the signal regions. We generate simulated samples with Madgraph5 [20], perform showering and hadronization with Pythia [21] and simulate the CMS detector response using Delphes [22], with additional 20% relative smearing of the  $E_T^{\text{miss}}$  to account for multiple in-

interactions. We validate our calculations by reproducing the predicted yields for the two dominant backgrounds, SM  $t\bar{t} \rightarrow \ell\nu bqq'b$  and SM  $t\bar{t} \rightarrow \ell\nu b\ell'\nu b$ , in each of the signal regions. Distributions of reconstructed quantities for an example signal sample and  $t\bar{t}$  backgrounds are shown in Fig 2. Note that the  $M_{T2}^W$  distribution demonstrates significant power in discriminating between SM  $t\bar{t}$  and  $t\bar{t}H$ .

We calculate upper bounds on  $\sigma(t\bar{t}H) \times BF(H \rightarrow \text{inv.})$  using a one-sided profile likelihood and the CLs technique [23, 24], evaluated using the asymptotic approximation [25]. For each of the sixteen signal regions, we calculate the median expected limit on  $\sigma(t\bar{t}H) \times BF(H \rightarrow \text{inv.})$ . The region with the strongest expected limit is that targeting  $\tilde{t} \rightarrow t\tilde{\chi}$  in the high- $\Delta M$  regime, with  $E_T^{\text{miss}} > 250$  GeV. This region has the additional requirements of  $\min(\Delta\phi[E_T^{\text{miss}}, j]) > 0.8$ ,  $M_{T2}^W > 200$  GeV and  $\chi_{\text{had}}^2 < 5.0$ . The expected background is reported to be  $9.5 \pm 2.8$ . With our simulated sample, we calculate an expected  $t\bar{t}H$  yield of 11.4 events if  $BF(H \rightarrow \text{inv.}) = 1.0$ . The efficiency of this selection for  $t\bar{t}H \rightarrow t\bar{t}\chi\bar{\chi}$  events with  $m_H = 125$  GeV is 0.45%, with no appreciable dependence on  $m_\chi$  up to  $m_\chi = m_h/2$ .

In this particular signal region, the data have fluctuated quite low,  $N_{\text{obs}} = 3$  events, giving an observed upper bound considerably stronger than the median expected results; see Fig 3. Dividing by the predicted rate of  $t\bar{t}H$  production in the SM [26] gives a limit on  $BF(H \rightarrow \text{inv.})$ ; the observed (expected) result is  $< 0.40$  (0.65) at 95% CL for  $m_H = 125$  GeV.

It is worth mentioning that by quoting a limit directly on  $BF(H \rightarrow \text{inv.})$ , we have made the strong assumption that the rate of  $t\bar{t}H$  is unchanged with respect to its SM value. The  $t\bar{t}H$  production mode has been searched for by CMS in a variety of decay modes [27], and while consistent with the SM expectation, it does currently show an excess. Similarly, ATLAS finds an excess in the four lepton decay mode that is consistent with a slight excess in a combination of the gluon fusion, vector boson fusion, and  $t\bar{t}H$  channels, but is consistent with the SM [28]. In the case that the  $t\bar{t}H$  rate turns out to be larger (smaller) than the SM expectation, our limits will become correspondingly stronger (weaker). The situation clearly highlights the importance of an independent direct determination of the  $t\bar{t}H$  rate through a visible Higgs boson decay mode.

We combine all current published results to calculate the global limit from direct searches; a summary of the datasets are given in Table I. We treat each channel as a simple counting experiment from the total signal yields reported, as per-bin estimates and uncertainties are not provided. We divide the uncertainties into categories which are correlated or uncorrelated across channels. Assumptions about the fraction of correlated versus uncorrelated uncertainties has a minor ( $< 5\%$  relative) effect on the observed limit.

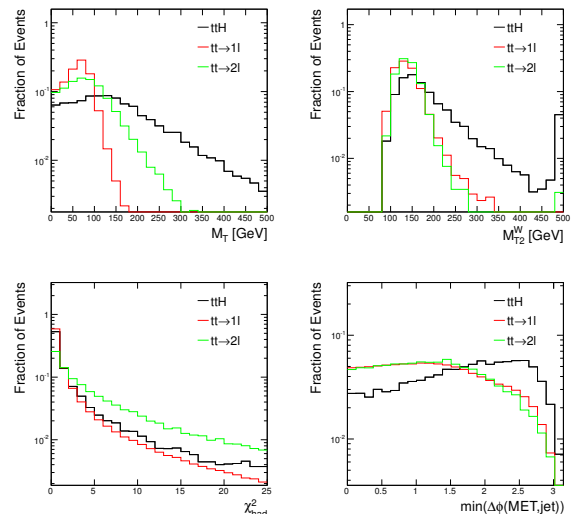


FIG. 2: Kinematics of  $t\bar{t}H$  with  $H \rightarrow \text{invisible}$  and all  $t\bar{t}$  decay modes, compared to the two dominant backgrounds, SM top quark production with either single lepton ( $\ell\nu bqq'b$ ) or di-lepton ( $\ell\nu b\ell'\nu b$ ) decay modes. Distributions are shown of  $M_T$ , the transverse mass;  $M_{T2}^W$ , as defined in Ref. [19];  $\chi_{\text{had}}^2$ , the consistency of the  $jjb$  system with a top quark hadronic decay; and  $\min(\Delta\phi[\text{MET}, \text{jet}])$ , the minimum angle between the  $E_T^{\text{miss}}$  and any jet. Distributions are shown after requiring exactly one lepton, at least four jets and one  $b$ -tag.

We attempt to reproduce the results quoted by the experiments in each channel; see Table II. In channels where multiple bins have been used, not enough information has been provided to reproduce the results. Our treatment, which groups all of the bins together, suffers from some degradation of statistical power as expected. However, even in cases where the experimental result is done with a single bin, for example the CMS vector-boson-fusion  $qqH$  which is the most powerful single channel other than  $t\bar{t}H$ , we are not able to exactly reproduce the results quoted in the paper due to some unreported correlations of systematic uncertainties in the publication; the difference is less than 20%. As the  $t\bar{t}H$  channel is the strongest result, these discrepancies have essentially no impact on the final result.

The final combination yields an observed (expected) result of  $BF(H \rightarrow \text{inv.}) < 0.40$  (0.40) at 95% CL for  $m_H = 125$  GeV.

If the primary interaction of dark matter with the SM is via the Higgs boson (the ‘‘Higgs Portal’’ [31]), the bound on invisible decays of the Higgs boson can be translated directly into the properties of dark matter such as its elastic scattering with nuclei [4–6]. The bound on the partial width into invisible states implies an upper bound on the Higgs boson coupling to dark matter, and thus the scattering cross section. In Figure 4, we show the translation of the bound  $BF(H \rightarrow \text{inv.}) < 0.40$  onto the spin-independent scattering cross section with

TABLE I: Summary of datasets used in combined limits. The expected backgrounds, uncertainties and observed yields are taken from the experimental results. The expected signal yields are quoted for  $\sigma(m_H = 125)$ ,  $\text{BF}(H \rightarrow \text{inv.}) = 1.0$ . In all cases other than  $t\bar{t}H$  expected signal yields are taken from the experimental results; for  $t\bar{t}H$ , it is due to our calculation in simulated samples.

Exp.	Mode	Dataset	Background	Obs.	Signal
ATLAS [11]	$Zh \rightarrow \ell\ell + E_T^{\text{miss}}$	7 TeV	$25.4 \pm 1.9$	28	8.9
	$Zh \rightarrow \ell\ell + E_T^{\text{miss}}$	8 TeV	$138 \pm 10$	152	44
CMS [12]	$Zh \rightarrow \ell\ell + E_T^{\text{miss}}$	7 TeV	$19.7 \pm 9.8$	19	5.4
	$Zh \rightarrow \ell\ell + E_T^{\text{miss}}$	8 TeV	$89.0 \pm 8.5$	82	25.0
	$Zh \rightarrow \ell\ell + j + E_T^{\text{miss}}$	7 TeV	$5.4 \pm 1.6$	5	0.9
	$Zh \rightarrow \ell\ell + j + E_T^{\text{miss}}$	8 TeV	$24.4 \pm 10.0$	28	4.1
CMS[12]	$Zh \rightarrow b\bar{b} + E_T^{\text{miss}}$	8 TeV, low $p_T^H$	$40.5 \pm 4.1$	38	1.6
	$Zh \rightarrow b\bar{b} + E_T^{\text{miss}}$	8 TeV, med $p_T^H$	$64.8 \pm 181.3$	61	3.6
	$Zh \rightarrow b\bar{b} + E_T^{\text{miss}}$	8 TeV, high $p_T^H$	$181.3 \pm 9.8$	204	12.6
CMS[12]	$qqH \rightarrow jj + E_T^{\text{miss}}$	8 TeV	$332 \pm 58$	390	224
CMS recast[18]	$t\bar{t}H \rightarrow 1\ell + 4j + E_T^{\text{miss}}$	8 TeV	$9.5 \pm 2.8$	3	11.4

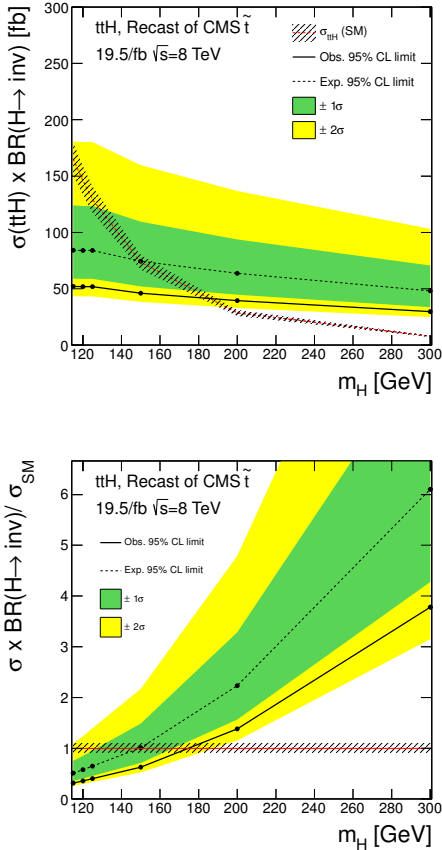


FIG. 3: Top pane gives 95% CL upper limits on  $\sigma(t\bar{t}H) \times \text{BF}(H \rightarrow \text{inv.})$ , including both expected and observed limits. Also shown is the SM rate of  $\sigma(t\bar{t}H)$  [26]. The bottom pane shows the ratio of the constraint to the SM  $\sigma(t\bar{t}H)$  cross section.

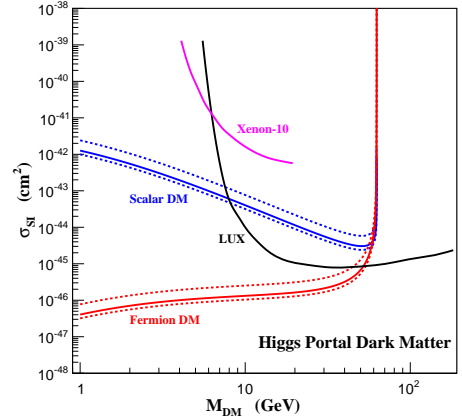


FIG. 4: Translation of the bound on  $\text{BF}(H \rightarrow \text{inv.}) < 0.40$  into a constraint on the spin-independent scattering of Higgs portal dark matter with nucleons, for scalar DM (solid blue curves) and fermion DM (solid red curves). The envelope around each constraint represents the uncertainty in the hadronic matrix elements. Also shown are constraints from LUX [29] and Xenon-10 [30].

nucleons ( $\sigma_{\text{SI}}$ ). The translation relies on the matrix elements  $\langle \sum_q m_q \bar{q}q \rangle = 0.33^{+0.3}_{-0.7} m_N$ , as determined by lattice QCD [32]; solid lines correspond to the central value, and the dashed lines show the envelope within these uncertainties. Also shown for comparison are the current limits on  $\sigma_{\text{SI}}$  from the LUX [29] and Xenon-10 [30] experiments. The comparison shows the familiar behavior where high energy searches very effectively probe low dark matter masses, whereas the direct searches are more effective for larger mass dark matter [33–35], particularly for  $M_{\text{DM}} > m_H/2$ , where on-shell Higgs bosons are too

TABLE II: Observed and expected limits at 95%CL on  $\text{BF}(H \rightarrow \text{inv.})$  in each channel and combinations. Note these are our analysis of the reported results as single-bin experiments, and so in some cases are slightly weaker than the reported results.

Exp.	Mode	Obs. (Exp.) limit
ATLAS [11]	$Zh \rightarrow \ell\ell + E_{\text{T}}^{\text{miss}}$	1.04 (0.81)
CMS [12]	$Zh \rightarrow \ell\ell + E_{\text{T}}^{\text{miss}}$	1.02 (1.19)
CMS [12]	$Zh \rightarrow b\bar{b} + E_{\text{T}}^{\text{miss}}$	3.15 (2.69)
CMS [12]	$qqH \rightarrow jj + E_{\text{T}}^{\text{miss}}$	0.76 (0.57)
CMS recast[18]	$t\bar{t}H \rightarrow \ell\ell 4j + E_{\text{T}}^{\text{miss}}$	0.40 (0.65)
CMS[12, 18]	$qqH + t\bar{t}H$	0.45 (0.47)
All[11, 12]	All but $t\bar{t}H$	0.63 (0.46)
All[11, 12, 18]	All	0.40 (0.40)

light to decay into dark matter.

The limits presented here rely on the reinterpretation of a  $t\bar{t} + E_{\text{T}}^{\text{miss}}$  sample originally selected in order to optimize sensitivity to  $t\bar{t}\tilde{\chi}$  rather than  $t\bar{t}H$ . A dedicated study may yield stronger limits, but we expect such improvements to be modest for two reasons. First, the variables used to search for  $t\bar{t}\tilde{\chi}$  also have power to discriminate between  $t\bar{t}H$  and the major backgrounds; see Fig. 2. Second, a rough optimization for  $t\bar{t}H$  has already been done here, with respect to the large number of signal regions provided in the CMS result.

To summarize, we report the first limit on invisible Higgs boson decays in the  $t\bar{t}H$  production mode, which currently yields the strongest individual limit on the Higgs decay to dark matter particles. In addition, we provide a combination of all available experimental limits and show the implications for theories where dark matter interacts with the SM primarily via the Higgs boson.

### Acknowledgements

The authors are grateful to P.J. Fox and Kyle Cranmer for reading the manuscript. NZ and DW are supported by the Department of Energy, Office of Science. ZK is supported by the UC Irvine SURP program. The research of TMPT is supported in part by NSF grant PHY-1316792 and by the University of California, Irvine through a Chancellor's Fellowship.

---

[1] G. Aad et al. (ATLAS Collaboration), Phys.Lett. **B716**, 1 (2012), 1207.7214.  
[2] S. Chatrchyan et al. (CMS Collaboration), Phys.Lett. **B716**, 30 (2012), 1207.7235.  
[3] G. Belanger, F. Boudjema, A. Cottrant, R. Godbole, and A. Semenov, Phys.Lett. **B519**, 93 (2001), hep-ph/0106275.  
[4] S. Kanemura, S. Matsumoto, T. Nabeshima, and N. Okada, Phys.Rev. **D82**, 055026 (2010), 1005.5651.

[5] P. J. Fox, R. Harnik, J. Kopp, and Y. Tsai, Phys.Rev. **D85**, 056011 (2012), 1109.4398.  
[6] A. Djouadi, O. Lebedev, Y. Mambrini, and J. Quevillon, Phys.Lett. **B709**, 65 (2012), 1112.3299.  
[7] A. Djouadi, A. Falkowski, Y. Mambrini, and J. Quevillon, Eur.Phys.J. **C73**, 2455 (2013), 1205.3169.  
[8] G. F. Giudice, R. Rattazzi, and J. D. Wells, Nucl.Phys. **B595**, 250 (2001), hep-ph/0002178.  
[9] G. Servant and S. Tulin, Phys.Rev.Lett. **111**, 151601 (2013), 1304.3464.  
[10] G. Aad et al. (ATLAS Collaboration), Phys.Rev.Lett. **112**, 041802 (2014), 1309.4017.  
[11] G. Aad et al. (ATLAS Collaboration), Phys.Rev.Lett. **112**, 201802 (2014), 1402.3244.  
[12] S. Chatrchyan et al. (CMS Collaboration) (2014), 1404.1344.  
[13] L. H. W. for Higgs boson searches (ALEPH Collaboration, DELPHI Collaboration, CERN-L3 Collaboration, OPAL Collaboration) (2001), hep-ex/0107032.  
[14] G. Belanger, B. Dumont, U. Ellwanger, J. Gunion, and S. Kraml, Phys.Rev. **D88**, 075008 (2013), 1306.2941.  
[15] J. Ellis and T. You, JHEP **1306**, 103 (2013), 1303.3879.  
[16] P. P. Giardinio, K. Kannike, I. Masina, M. Raidal, and A. Strumia, JHEP **1405**, 046 (2014), 1303.3570.  
[17] S. Chatrchyan et al. (CMS Collaboration), JHEP **1306**, 081 (2013), 1303.4571.  
[18] S. Chatrchyan et al. (CMS Collaboration), Eur.Phys.J. **C73**, 2677 (2013), 1308.1586.  
[19] Y. Bai, H.-C. Cheng, J. Gallicchio, and J. Gu, JHEP **1207**, 110 (2012), 1203.4813.  
[20] J. Alwall, M. Herquet, F. Maltoni, O. Mattelaer, and T. Stelzer, JHEP **1106**, 128 (2011), 1106.0522.  
[21] T. Sjostrand, S. Mrenna, and P. Z. Skands, JHEP **0605**, 026 (2006), hep-ph/0603175.  
[22] J. de Favereau et al. (DELPHES 3), JHEP **1402**, 057 (2014), 1307.6346.  
[23] A. L. Read, J.Phys. **G28**, 2693 (2002).  
[24] T. Junk, Nucl.Instrum.Meth. **A434**, 435 (1999), hep-ex/9902006.  
[25] G. Cowan, K. Cranmer, E. Gross, and O. Vitells, Eur.Phys.J. **C71**, 1554 (2011), 1007.1727.  
[26] S. Heinemeyer et al. (LHC Higgs Cross Section Working Group) (2013), 1307.1347.  
[27] V. Khachatryan et al. (CMS Collaboration) (2014), 1408.1682.  
[28] G. Aad et al. (ATLAS Collaboration) (2014), 1408.5191.  
[29] D. Akerib et al. (LUX Collaboration), Phys.Rev.Lett. **112**, 091303 (2014), 1310.8214.  
[30] J. Angle et al. (XENON10 Collaboration), Phys.Rev.Lett. **107**, 051301 (2011), 1104.3088.  
[31] C. Burgess, M. Pospelov, and T. ter Veldhuis, Nucl.Phys. **B619**, 709 (2001), hep-ph/0011335.  
[32] D. Toussaint and W. Freeman (MILC Collaboration), Phys.Rev.Lett. **103**, 122002 (2009), 0905.2432.  
[33] J. Goodman, M. Ibe, A. Rajaraman, W. Shepherd, T. M. Tait, et al., Phys.Rev. **D82**, 116010 (2010), 1008.1783.  
[34] Y. Bai, P. J. Fox, and R. Harnik, JHEP **1012**, 048 (2010), 1005.3797.  
[35] J. Goodman, M. Ibe, A. Rajaraman, W. Shepherd, T. M. Tait, et al., Phys.Lett. **B695**, 185 (2011), 1005.1286.